



Identification of novel series of pyrazole and indole-urea based DFG-out PYK2 inhibitors

Samit K. Bhattacharya^{a,*}, Gary E. Aspnes^a, Scott W. Bagley^a, Markus Boehm^a, Arthur D. Brosius^a, Leonard Buckbinder^c, Jeanne S. Chang^d, Joseph Dibrino^a, Heather Eng^b, Kosea S. Frederick^b, David A. Griffith^a, Matthew C. Griffor^d, Cristiano R. W. Guimarães^a, Angel Guzman-Perez^a, Seungil Han^d, Amit S. Kalgutkar^b, Jacquelyn Klug-McLeod^a, Carmen Garcia-Irizarry^a, Jianke Li^a, Blaise Lippa^a, David A. Price^{a,*}, James A. Southers^a, Daniel P. Walker^a, Liuqing Wei^a, Jun Xiao^a, Michael P. Zawistoski^a, Xumiao Zhao^a

^aWorldwide Medicinal Chemistry, Pfizer Global Research and Development, 620 Memorial Drive, Cambridge, MA 02139, United States

^bPharmacokinetics, Dynamics and Metabolism, Pfizer Global Research and Development, 620 Memorial Drive, Cambridge, MA 02139, United States

^cCardiovascular and Metabolic Diseases Research Unit, Pfizer Global Research and Development, 620 Memorial Drive, Cambridge, MA 02139, United States

^dStructural Biology & Biophysics, Pfizer Global Research and Development, Eastern Point Road, Groton, CT 06340 United States

ARTICLE INFO

Article history:

Received 6 August 2012

Revised 2 October 2012

Accepted 8 October 2012

Available online 16 October 2012

Keywords:

PYK2

FAK

DFG-out

Osteoporosis

Kinase inhibitor

BIRB-796

ABSTRACT

Previous drug discovery efforts identified classical PYK2 kinase inhibitors such as **2** and **3** that possess selectivity for PYK2 over its intra-family isoform FAK. Efforts to identify more kinome-selective chemical matter that stabilize a DFG-out conformation of the enzyme are described herein. Two sub-series of PYK2 inhibitors, an indole carboxamide-urea and a pyrazole-urea have been identified and found to have different binding interactions with the hinge region of PYK2. These leads proved to be more selective than the original classical inhibitors.

© 2012 Elsevier Ltd. All rights reserved.

There is an unmet need in the osteoporosis field for new treatment options beyond the current mainstay of anti-resorptive therapeutics such as bisphosphonates, an anti-RANKL antibody, and estrogen receptor modulators (SERMs).¹ While these treatments have vastly improved the quality of life of patients, they have significant drawbacks. Bisphosphonates have safety concerns including increased risk of cancer, atrial fibrillation, and musculoskeletal pain. More recently, osteonecrosis of the jaw has emerged as a relatively rare but devastating adverse effect.² In addition, there is a dosing inconvenience whereby after oral administration the patient is required to be seated in an upright posture for up to an hour post dosing. Furthermore, from an efficacy standpoint, both the bisphosphonates and SERMs are antiresorptive and not bone anabolic. Therefore they do not restore bone in chronically osteoporotic patients.

The only currently approved anabolic agent, recombinant human parathyroid hormone,³ is limited to use in the most severely afflicted patients because of concerns for osteosarcoma and its requirement for daily injections.

Within the osteoporosis literature there have been recent publications disclosing the potential of proline-rich kinase 2 (PYK2) as a molecular target for improving bone formation. PYK2 and focal adhesion kinase (FAK) are non receptor tyrosine kinases and together constitute the FAK subfamily.⁴ FAK is ubiquitously expressed; however, PYK2 expression is highest in the brain and hematopoietic system.

Initial studies using PYK2 knock-out female mice exhibited the skeletal phenotype of higher bone mass and mineral density when compared to wild type animals.⁵ The mice were viable and fertile. Spurred on by these initial findings, small molecule modulators were designed and tested for efficacy. They increased bone formation and protected against bone loss in ovariectomized rats, an established model of postmenopausal osteoporosis. These studies suggested that selective modulation of this kinase may offer an

* Corresponding authors. Tel.: +1 617 551 3177.

E-mail address: samit.k.bhattacharya@pfizer.com (S.K. Bhattacharya).

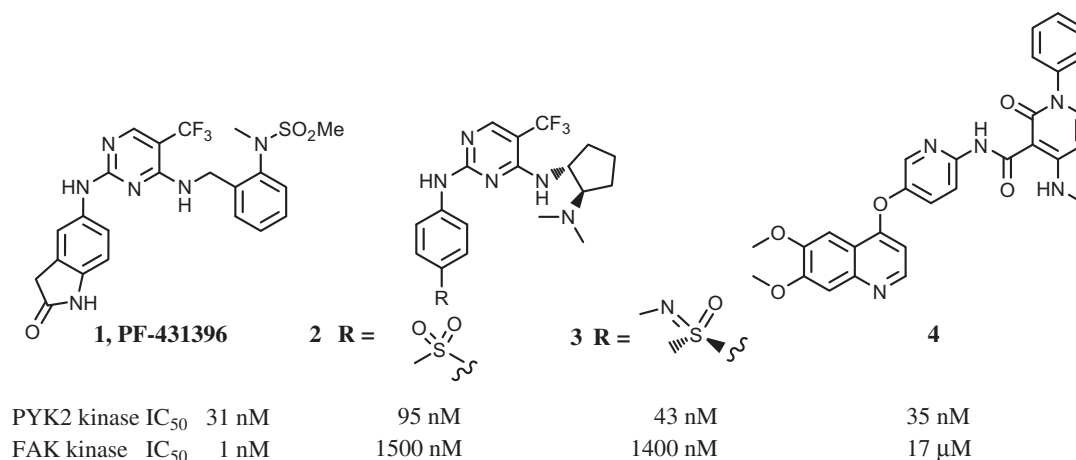


Figure 1. Representative PYK2 kinase inhibitors in literature.

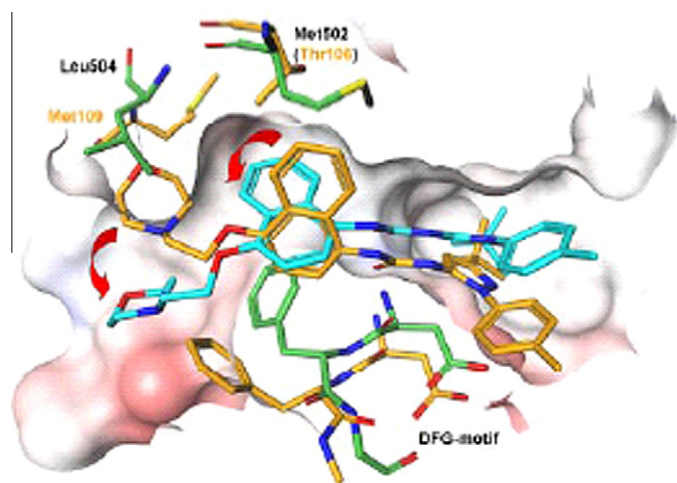


Figure 2. Binding modes of BIRB-796 bound to PYK2 (blue) and p38 (yellow).

opportunity to deliver an orally available anabolic therapy for the treatment of osteoporosis.

These aforementioned small molecule modulators were classical kinase inhibitors that make a hinge contact with the enzyme. The originally disclosed lead classical inhibitor, **1 (PF-431396)** was improved upon to arrive at analogs **2** and **3** in the same class that had better intra-family isoform selectivity versus FAK.⁶ (Fig. 1).

Broad selectivity across a kinase panel is often difficult to achieve with classical kinase inhibitors while inhibitors that stabilize the 'inactive' DFG-out conformation (these compounds move the DFG motif of the enzyme upon their binding and do not necessarily require the hinge contact)⁷ are relatively more selective.⁸ Thus we invested efforts at uncovering chemistry substrates that would be broadly defined as stabilizers of the DFG-out conformation. The current article describes these efforts that led to two sub-series of DFG-out leads for PYK2 and their selectivity profiles in a typical kinase selectivity panel. A recent publication has described chemical matter (**4**) that is DFG-in and is remarkably FAK selective.⁹

To look for leads that could help PYK2 adopt a DFG-out conformation we conducted targeted screening of known DFG-out inhibitors in the literature including imatinib, BIRB-796 (**5**), and sorafenib against PYK2 enzyme.⁵ As previously reported, **5** was identified as an active, albeit weak, PYK2 inhibitor (imatinib was inactive in the PYK2 assay).¹⁰ Slow-on/slow-off binding kinetics,

[determined using scintillation proximity resonance (SPR)], NMR experiments and ultimately an X-ray crystal structure demonstrated that BIRB-796 was a specific ligand for PYK2 and that it stabilized a 'DFG-out' conformation, despite its low affinity. Notably, the crystal structure revealed a PYK2 specific binding mode with significant differences from the published p38-BIRB796 (yellow, Fig. 2, PDB code: 1KV2) interaction. The naphthyl ring is rotated out of plane relative to p38-BIRB796, and the morpholino substituent in PYK2-BIRB796 (blue, Fig. 2, PDB code: 3FZS) complex does not interact with the hinge residues. Orientation of the tolyl-*tert*-butylpyrazole is well conserved.

Despite exquisite potency against p38, we chose to use BIRB-796 as an initial lead for medicinal chemistry efforts to develop a potent and selective DFG-out inhibitor of PYK2. It rapidly became evident that the tolyl-pyrazole fragment provided significant binding energy (as published for p38 inhibition).¹¹ Conversely, modification of the naphthyl group was tolerated and the PYK2 specific binding mode suggested selectivity and potency might be found through replacement of that moiety. Several compound libraries were targeted that aimed at replacement of the naphthyl group while holding the tolyl-pyrazole and urea constant. Two urea sub-series that emerged from this work were the indole carboxamides (**6**) and pyrazoles (**7**) which provided improvements in both potency and ligand efficiency (Fig. 3). Subsequent efforts were made

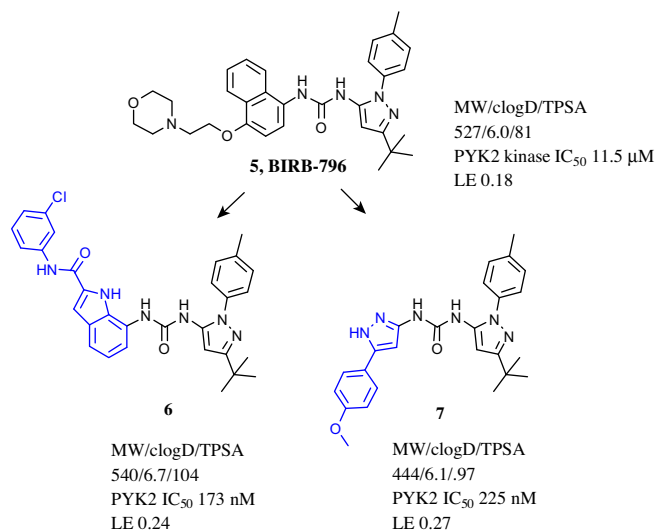
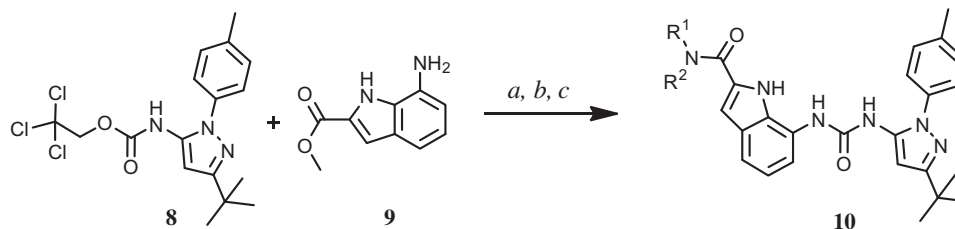


Figure 3. Two urea sub-series.



Scheme 1. (a) DMSO, DIPEA, 50 °C, 12 h, 81%; (b) 1 M NaOH, MeOH, 50 °C, ~2 h, 86%; (c) R¹R²NH, HATU, DIPEA, NMP, 50 °C, 4 h, ~98%. HATU = O-(7-azabenzotriazol-1-yl)-N,N,N',N'-tetramethyluronium hexafluorophosphate.

Table 1
Biological data for indole-carboxamide urea series

Entry	R ¹	R ²	MW	cLogD (eLogD ^a)	PYK2 kinase IC ₅₀ (nM) ^a	LE ^{a3}	PYK2 Cell IC ₅₀ (nM) ^b	HLM Clearance ml/min/kg	Dofetilide % inhibition @ 10 μM	FAK Kinase IC ₅₀ (nM)
10a			484	3.8	31 (<30 n = 2) ^{a2}	0.28	265	77	15	
10b	Me	H	444	5.2 (4.9)	1700 (3310, 870)	0.23	2780	28		
10c	iPr	H	472	6.0 (5.3)	78 (73, 83)	0.27	530 (438, 642)	93	3	7860
10d			539	0.35	57 ± 19 (n = 3)	0.24	7660	53	91	
10e	Me		549	4	398 ± 219 (n = 3)	0.22	553	53	31	>10000
10f		H	516	5.9	75 ± 40 (n = 5)	0.26	283	122	4	>10000

^aeLogD = measured LogD (at pH 7.4)

^a PYK2 fluorescence polarization (FP) protocol as described in Ref. 5 IC₅₀ values represent the concentration to inhibit 50% of the phosphorylation of a peptide substrate relative to vehicle control. Numbers indicate the IC₅₀ values generated from individual 8-point concentration response relationships in triplicate. Where n ≥ 3, the geometric mean and standard deviation is reported.

^{a2} Data generated in PYK2 FP 8-point assay (described above) with a higher top dose (100 μM instead of 10 μM).

^{a3} LE = ligand efficiency.

^b PYK2 LI-COR cellular assay (protocol has been published).¹³ Numbers indicate IC₅₀ values generated from 9-point concentration response relationships in quadruplicate. Where n ≥ 3, the geometric mean and standard deviation is reported.

^c Protocols for measuring half-lives in HLM and subsequent scaling to blood clearance have been published.¹⁴

^d [³H]-Dofetilide binding assay as described.¹⁵ Numbers indicate the percentage inhibition of [³H]-dofetilide binding to the hERG protein stably expressed on HEK-293 cells following a 10 μM dose of test compound.

^e FAK fluorescence polarization (FP) protocol as described in Ref. 5 using FAK kinase domain construct as described.¹⁶ IC₅₀ values represent the concentration to inhibit 50% of the phosphorylation of a peptide substrate relative to vehicle control. Numbers indicate IC₅₀ values generated from individual 8-point concentration response relationships in triplicate.

to improve the potency and physicochemical properties of each urea subseries in parallel.

Clearly the high molecular weight and lipophilicity of the indole carboxamide sub-series were liabilities and we sought to mitigate these through further optimization.¹² Amide libraries were designed in an effort to improve potency while reducing molecular weight and/or lipophilicity (some examples shown in Table 1). Template and library preparation is shown in Scheme 1. 7-Aminoindole-2-carboxylic methyl ester (**9**) was coupled with troc-amino-pyrazole (**8**) and the ester saponified to give an acid template which was coupled to various amines with HATU.

Several compounds with improved properties were found. Efforts to reduce molecular weight and improve ligand efficiency led to entries **10a**, **b** and **c**. While the simple methyl amide, **10b**, eroded PYK2 potency substantially, the corresponding isopropyl indole amide **10c** provided improved potency with reduced lipophilicity relative to the lead **6**. Other efforts to reduce the lipophilicity and/or increase solubility of these indoles led to entries **10d**, **10e** and **10f**. For the spiro-*bis*-pyrrolidine **10d**, while kinase potency was good, it showed a marked loss in cellular potency most probably because the basic amine affected cellular permeability. The other two entries, **10e** and **10f** had varying potency in the kinase assay, but similar cell potency to **10c** which suggested that these might be viable *in vivo* tools.

Some additional efforts were directed towards replacement of the indole motif. However, even conservative changes (e.g., imidazole/benzoxazole) greatly reduced activity (data not shown). Subsequent solution of an X-ray co-crystal structure with **10c** helped to provide a rationale for the importance of the indole carboxamide (see below).

While optimization was ongoing in the indole subseries, we also looked at the *bis*-pyrazole urea series. In the indole series, we had found the *tert*-butyl-pyrazole-tolyl group provided optimal potency and ligand efficiency (data not shown). Thus for the pyrazole series, we targeted exploration off the NH-pyrazole vector to maximize lipophilic efficiency.^{17,18} We utilized library and singleton chemistry to explore the 3-position of the NH-pyrazole (**13**, Scheme 2). The desired ureas were synthesized by reacting the common tolyl-pyrazole carbamate intermediate **11** with various aminopyrazoles under thermal conditions, as noted in Scheme 2.

As shown in Table 2, attaining good PYK2 activity in the *bis*-pyrazole urea series was challenged with high molecular weight and lipophilic chemical space. A pendant aryl group with a hydrogen bond acceptor appeared critical for PYK2 potency, for reasons which would become evident from X-ray data (*vide infra*). Subsequent modifications were directed towards decreasing lipophilicity while maintaining an appropriate H-bond acceptor. The phenyl group in **7** (or **13a**) was replaced with pyridines and diazines in or-

der to lower the LogD. Addition of nitrogen *ortho* to the pyrazole was deleterious for PYK2 kinase potency (**13b** and **13d**), while the *meta*-pyridyl isomer, **13c**, was nearly equipotent. The corresponding pyridone, **13e**, had better physicochemical properties but while PYK2 kinase potency was improved, cell potency was substantially reduced, presumably due to permeability issues. Sim-

ilar to analogs **13b** and **13d**, addition of an *ortho*-nitrogen to give the pyridazinone analog **13f** led to reduced PYK2 potency. To remove the additional H-bond, the N-methylated pyridone **13g** was made but showed further loss in PYK2 kinase and cell potency.

A parallel effort was made to improve potency by increasing the H bond acceptor basicity and/or removing a rotatable bond by

Table 2
Biological data for bis-pyrazole urea series

Entry	R	MW	cLogD (eLogD ^a)	PYK2 kinase IC ₅₀ (nM) ^d	LE ^b	PYK2 Cell IC ₅₀ (nM) ^c	HLM Clearance ml/min/kg ^d	Dofetilide %Inhibition @ 10 (μM) ^e	FAK kinase IC ₅₀ (nM) ^f
13a		459	6.5	1200 ± 55 (n = 3)	0.24		129	7	4770
13b		445	5.2	3819 (3360, 4340)	0.24	607			>10000
13c		445	5.4 (4.9)	361 ± 30 (n = 3)	0.27	524 ± 191 (n = 3)	48	15	
13d		446	5.0	>10000 (n = 2)					
13e		431	3.75 (3.7)	141 ± 28 (n = 3)	0.29	4.7 ± 2.1 μM (n = 3)	11.9	36	
13f		432	0.75	1350 ^{a2}	0.26	3.6 ± 1.1 μM (n = 3)	16	24	
13g		445	4.1 (3.8)	429 (315, 585)	0.26	2.5 μM (1.8, 3.5)	20	30	
13h		472	5.7	69	0.28	328 (316, 342)	92	1	
13i		454	5.5 (4.5)	25 ± 41 (n = 4)	0.30	236 ± 33 (n = 3)	44	55	
13j		465	6.3 (5.2)	6.4 ± 3.7 (n = 4)	0.30	98 ± 78 (n = 4)	55	31	608
13k		466	5.4 (4.7)	12.5 ± 2.3 (n = 4)	0.30	62 (41, 94)	149	12	473
13l		445	4.9	637 ± 407 (n = 3)	0.26	190 ± 112 (n = 4)	109	16	>10000
13m		368	3.2	>100 μM ^{a3}					

^a eLogD = measured LogD (at pH 7.4)

^a PYK2 fluorescence polarization (FP) protocol as described in Ref. 5. IC₅₀ values represent the concentration to inhibit 50% of the phosphorylation of a peptide substrate relative to vehicle control. Numbers indicate IC₅₀ values generated from individual 8-point concentration response relationships in triplicate. Where n ≥ 3, the geometric mean and standard deviation is reported.

^{a2} Data generated in PYK2 FP 8-point assay (described above) with a higher top dose (100 μM instead of 10 μM).

^{a3} Single point data

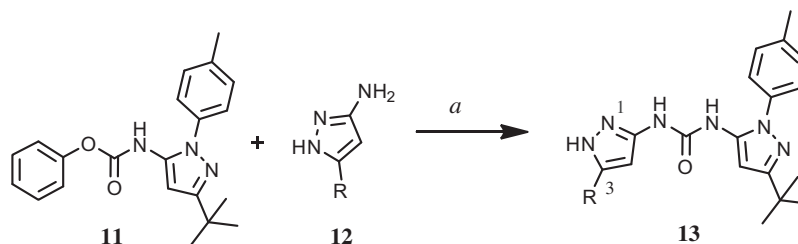
^b LE = ligand efficiency.

^c PYK2 LI-COR cellular assay (protocol as described in Ref. 13). Numbers indicate IC₅₀ values generated from 9-point concentration response relationships in quadruplicate. Where n ≥ 3, the geometric mean and standard deviation is reported.

^d Protocols for measuring half-lives in HLM and subsequent scaling to blood clearance have been published (see: Ref. 14).

^e [³H]-Dofetilide binding assay as described in Ref. 15. Numbers indicate the percentage inhibition of [³H]-dofetilide binding to the hERG protein stably expressed on HEK-293 cells following a 10 μM dose of test compound.

^f FAK fluorescence polarization (FP) protocol as described in Ref. 5 using FAK kinase domain construct as described in Ref. 16. IC₅₀ values represent the concentration to inhibit 50% of the phosphorylation of a peptide substrate relative to vehicle control. Numbers indicate IC₅₀ values generated from individual 8-point concentration response relationships in triplicate



Scheme 2. (a) K_2CO_3 , THF, 80 °C, 16 h, ~80%.

replacing the anisole with heterobicyclic groups (**13h–k**). These analogs provided a 3–10 \times boost in PYK2 potency although they are at the edges of desired physicochemical properties. **13l** was made in an effort to improve physical properties by conceptually breaking the proximal ring of quinoline analog **13j**. Though LogD was reduced, the additional flexibility in **13l** resulted in decreased PYK2 potency and increased clearance (compared to **13j**). Further truncation to the hydroxymethyl compound **13m**, led to near complete loss of PYK2 activity, highlighting the need for an appropriate H bond acceptor in this series. While entry **13k** had the best lipophilic efficiency (LipE = 2.3)¹⁷ in this sub-series, entry **13j**¹⁹ provided a lead (LipE = 1.5) that had an acceptable overall profile in terms of PYK2 activity and ADME properties (as exemplified by moderate clearance in human liver microsomes, moderate hERG inhibition (as evidenced by dofetilide binding assay) and lack of competitive DDI versus CYP3A4, CYP2D6, CYP2C9 or CYP1A2).

Crystallographic analysis on both the *bis*-pyrazole and the indole carboxamide urea leads revealed different binding modes for these two sub-series. The crystal structure of pyrazole **13a** revealed that the methoxy oxygen has a hydrogen bond interaction with the amide backbone of Tyr505 in the hinge region, providing a rationale for the apparently critical H-bond acceptors in analogs **13a–m**. The pyrazole moiety is sandwiched by Met502 (gatekeeper residue) and Phe568 (DFG motif). One of the pyrazole nitrogens has a hydrogen bond (H-bond) interaction with Lys457. In contrast, there was no interaction with the hinge region present in the co-crystal structure of indole **10c** in PYK2. The indole nitrogen is involved in a water mediated H-bond interaction with Lys457 and Glu474. The isopropyl amide moiety at C2 position of the indole is involved in van der Waals contacts with Gly-rich loop.

Thus both sub-series *do induce a DFG-out conformation* of PYK2. However as shown in Fig. 4, the indole sub-series does not make any contact with the hinge region while the pyrazole analog with an appropriate substituent is able to reach to the hinge backbone.²⁰

The fact that indole carboxamide **10c** was able to give good potency without interaction with the hinge backbone gave us encour-

agement for a path toward kinase selectivity without requiring hinge interactions. This was realized, as in contrast to the classical kinase inhibitor, **1**, the indole carboxamide leads (entries **10c**, **10e** and **10f**, Table 1) were very selective versus FAK kinase. The *bis*-pyrazole urea leads were also selective against FAK but not as selective as the indole leads. This trend of kinase selectivity was evidenced when tested in a kinase selectivity panel at 1 μ M. As expected the indole-carboxamide urea series which does not make a hinge-contact has a better selectivity profile over the *bis*-pyrazole urea series. In general, both DFG-out lead series possessed improved kinase selectivity in comparison to the classical kinase inhibitor **1** as shown in the heat map below (Fig. 5).²¹ Although the starting lead (BIRB-796) for this current work was a potent p38 α inhibitor, both the pyrazole and the indole series show selectivity for p38 α (MAPK14). Similar to the trend of FAK selectivity, the indole carboxamides exhibit better selectivity than the pyrazoles.

The X-ray crystal data for **13a** suggested one additional potential avenue to optimize potency and permeability in the *bis*-pyrazole series. The observed H-bond between the pyrazole-N and Lys457 highlighted potential tautomerism in the pyrazole-NH motif and the possibility to eliminate a hydrogen-bond donor in order to improve permeability. Computational investigation of the tautomeric equilibrium in water revealed that the tautomer in the bound state (where the NH of the pyrazole is proximal to the NH of the urea), suggested by the hydrogen bond network in the crystal structure, is not the most stable one in solution. An energy penalty of +1.85 kcal/mol against the binding of **7** due to the tautomeric equilibrium was estimated by a combination of conformational analysis in solution and quantum mechanical calculations. These calculations suggested that an alternative heterocycle with no associated tautomerism could potentially have a 20-fold gain in potency if all contributions to binding were kept the same. To test this hypothesis and remove an H-bond to improve permeability, we made the isomeric pyrazole analogs, **13n** and **13o**. Indeed the pyrazole isomer, **13n**, where the distal N (from the urea) is methylated leaving the other N unencumbered to make the critical interaction with Lys457 was potent while

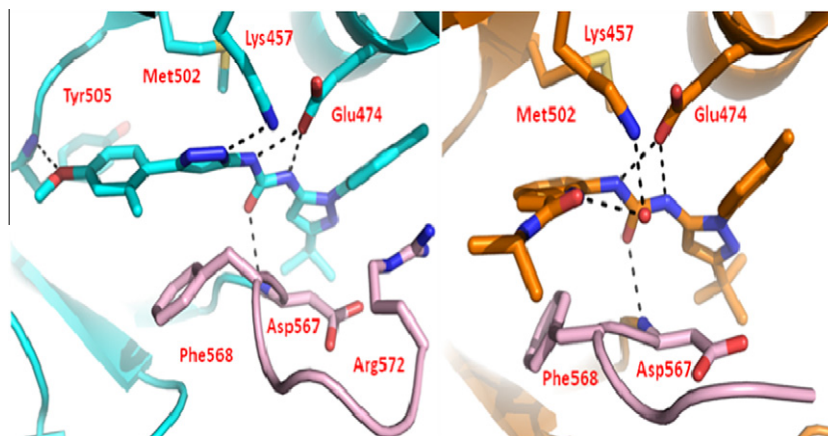


Figure 4. Crystal Structures of pyrazole **13a** and indole **10c**.

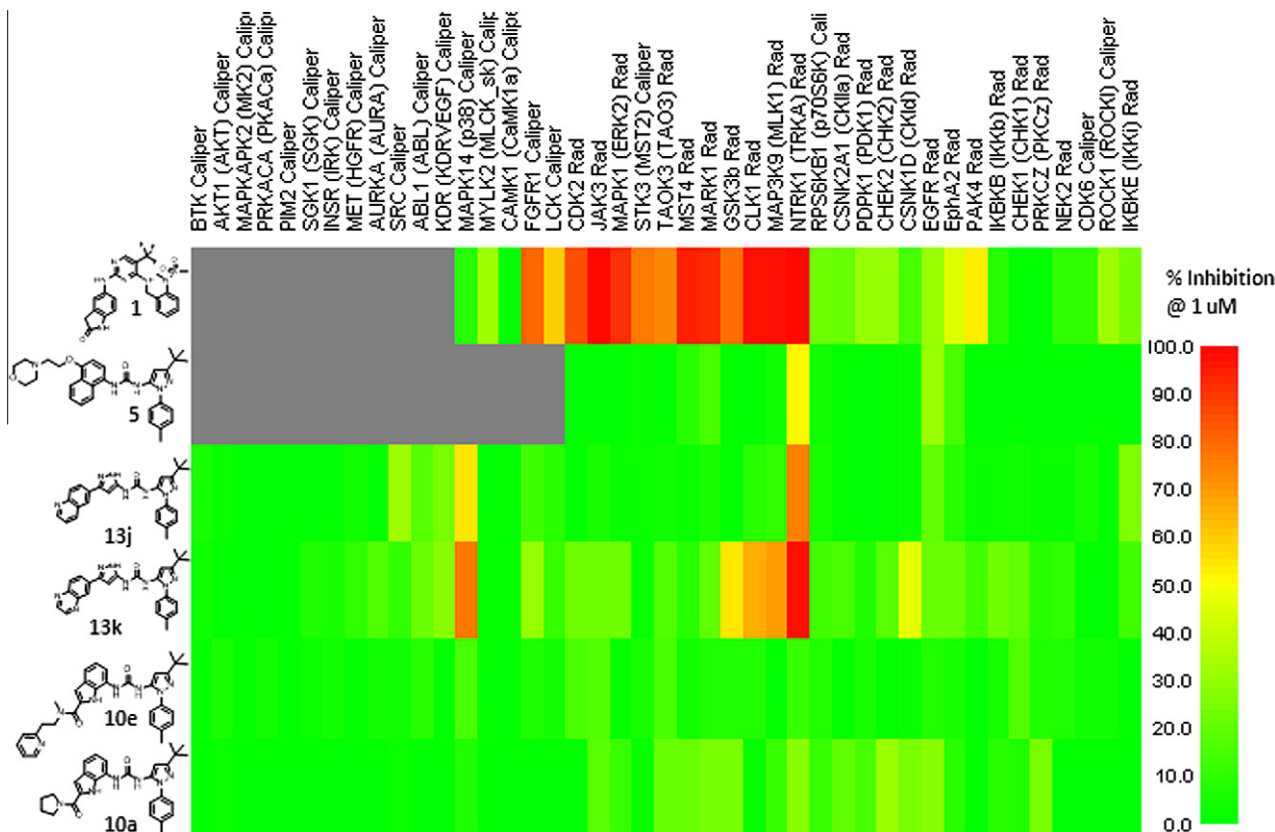


Figure 5. Kinase selectivity screen for representative analogs at 1 μM dose.

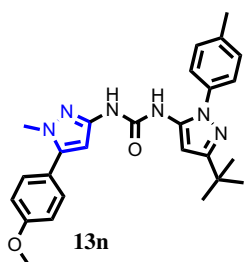
Table 3
Rat Pharmacokinetic Data for Selected Analogs^a

Entry	Compound	Series	Route	Dose	$t_{1/2}$ ^b	Cl_p (ml/min/kg)	Vd_{ss} (L/kg)	C_{max} (nM)	Calc C_{max} free (nM)	%F	PPB (fu)
1	10e	Indole urea	IV	1	2.2 ± 0.9	3.2 ± 1.3	0.4 ± 0.06	38265 ± 10396	25	69 ± 12	0.00066
			PO	30							
2	10f	Indole urea	IV	1	4.1 ± 2.6	4.8 ± 0.9	0.7 ± 0.2	621, 784	42	1.6 (1.5, 1.7)	0.06
			PO	30							
3	13j	Pyrazole urea	IV	1	2.0 (2.6, 1.5)	2.0 (1.8, 2.1)	0.15 (0.18, 0.12)	61324 (60142, 62505)	184	47	0.003
			PO	30							
4	13k	Pyrazole urea	IV	n/a	n/a						0.016
			PO	100	7.3 (3.7, 10.9)			68 (84, 52)	1.1	n/a	

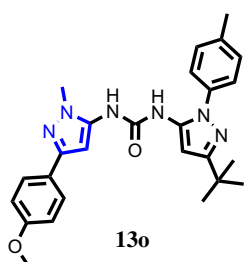
^a Pharmacokinetic studies were conducted in male Wistar-Han rats ($n = 2-3$). In cases where two animals were used, individual pharmacokinetic parameters are also depicted in parenthesis. Compounds were administered in 10% DMSO: 40% water :50% PEG400 for oral (PO) and intravenous (IV) studies.

^b Half-life $t_{1/2}$ values represent the terminal elimination (β) phase.

the corresponding isomer **13o** where the N closer to the urea is methylated is devoid of activity pointing to the significance of pyrazole N- Lys457 interaction.



PK2 kinase IC_{50} 360 nM
LE 0.26
PK2 cell IC_{50} 381 nM



PK2 kinase $IC_{50} > 10$ uM

However it was intriguing that there was not much difference in activity between the NH-pyrazole (**7**) and its N-methylated counterpart (**13n**). Application of the physics-based scoring method MM-GB/SA²² indicated that the active tautomer of **7** binds to PYK2 more favorably than its N-methylated analog **13n** by -2.2 kcal/mol. This difference in binding energy is due to a water-mediated hydrogen bond between the pyrazole-NH in **7** and the backbone carbonyl of Phe568 (this water was explicitly included in the MM-GB/SA calculations). We hypothesize that the energy gain for **13n** due to elimination of the tautomeric penalty is almost completely offset by its less favorable interaction in the binding site compared to **7** and hence the equivalent potencies of **7** and **13n**. Unfortunately, further attempts to replace the pyrazole with other 5-membered heterocycles (e.g., oxazole, isoxazole, thiazole, oxadiazole etc.) where there would be no tautomeric penalty did not yield better leads (data not shown).

We have previously reported on a functional osteogenesis assay in hMSC cultures.^{4,8} The classical inhibitor **1** led to modest increases in alkaline phosphatase activity but only when dosing was restricted to days 4–7. Compound-treated cells appeared to be stressed and the cultures did not mineralize, a finding that was attributed to the off-target activity of **1**. In contrast, **13j** and other DFG-out analogs such as **13i** showed a dose-dependent increase in both alkaline phosphatase activity and mineralization for a period of 14 days (as reported earlier),^{10,13} consistent with their improved selectivity.

In order to evaluate the *in vivo* pharmacokinetic properties, a few of the leads from both sub-series were advanced in rat oral bioavailability studies as tabulated in Table 3.

Representatives from both urea subseries were orally available with low plasma clearance (Cl_p) and low steady state distribution volumes ($V_{d_{ss}}$). Despite excellent total plasma exposure (C_{max}), the high protein binding levels (displayed as fraction unbound in rat, rPPB) as a consequence of their higher lipophilicity meant that the free concentrations (calculated C_{max} free) were quite low. High doses of these compounds would be required for meaningful inhibition of PYK2, and thus these leads were not advanced further.

In summary, we have described our efforts to convert the archetypal DFG-out p38 inhibitor BIRB-796 into two DFG-out lead series (with and without hinge contacts) that are potent and selective for PYK2. Compounds from these series showed functional osteogenic activity and oral exposure in rats. The *bis*-pyrazole and indole carboxamide urea series leads displayed surprisingly different modes in which they bind to PYK2 in a DFG-out conformation leading to one sub-series that is more selective than the other.

References and notes

- (a) Allen, J. G.; Fotsch, C.; Babij, P. *J. Med. Chem.* **2010**, 4332; (b) Lewiecki, E. M. *Cleve. Clin. J. Med.* **2009**, 76, 457.
- (a) Kanis, J. A.; Reginster, J.-Y.; Kaufman, J.-M.; Ringe, J.-D.; Adachi, J. D.; Hilgsmann, M.; Rizzoli, R.; Cooper, C. *Osteoporos. Int.* **2012**, 23, 213; (b) Khosla, S.; Bilezikian, J. P.; Dempster, D. W.; Lewiecki, M.; Miller, P. D.; Neer, R. M.; Recker, R. R.; Shane, E.; Shoback, D.; Potts, J. T. *J. Clin. Endocrinol. Metab.* **2012**, 2272.
- Canalis, E.; Giustina, A.; Bilezikian, J. P. *N. Engl. J. Med.* **2007**, 357, 905.
- Lipinski, C. A.; Loftus, J. C. *Expert Opin. Ther. Targets* **2010**, 14, 95.
- Buckbinder, L.; Crawford, D. T.; Qi, H.; Ke, H.-Z.; Olson, L. M.; Long, K. R.; Bonnette, P. C.; Baumann, A. P.; Hambor, J. E.; Grasser, W. A.; Pan, L. C.; Owen, T. A.; Luzzio, M. J.; Hulford, C. A.; Gebhard, D. F.; Paralkar, V. M.; Simmons, H. A.; Kath, J. C.; Roberts, W. G.; Smock, S. L.; Guzman-Perez, A.; Brown, T. A.; Li, M. *Proc. Natl. Acad. Sci. U.S.A.* **2007**, 104, 10619.
- (a) Walker, D. P.; Zawistoski, M. P.; McGlynn, M. A.; Li, J. C.; Kung, D. W.; Bonnette, P. C.; Baumann, A.; Buckbinder, L.; Houser, J. A.; Boer, J.; Mistry, A.; Han, S.; Xing, L.; Guzman-Perez, A. *Bioorg. Med. Chem. Lett.* **2009**, 19, 3253; (b) Walker, D. P.; Bi, F. C.; Kalgutkar, A. S.; Bauman, J. N.; Zhao, S. X.; Soglia, J. R.; Aspnes, G. E.; Kung, D. W.; Klug-McLeod, J.; Zawistoski, M. P.; McGlynn, M. A.; Oliver, R.; Dunn, M.; Li, J. C.; Richter, D. T.; Cooper, B. A.; Kath, J. C.; Hulford, C. A.; Autry, C. L.; Luzzio, M. J.; Ung, E. J.; Roberts, W. G.; Bonnette, P. C.; Buckbinder, L.; Mistry, A.; Griffor, M. C.; Han, S.; Guzman-Perez, A. *Bioorg. Med. Chem. Lett.* **2008**, 18, 6071.
- For a review on the field of DFG-out inhibitors, see: Liu, Y.; Gray, N. S. *Nat. Chem. Biol.* **2006**, 358.
- Davis, M. I.; Hunt, J. P.; Herrgard, S.; Ciceri, P.; Wodlicka, L. M.; Pallares, G.; Hocker, M.; Treiber, D. K.; Zarrinkar, P. P. *Nat. Biotechnol.* **2011**, 29, 1046.
- Allen, J. G.; Lee, M. R.; Han, C. Y.; Scherrer, J.; Flynn, S.; Boucher, C.; Zhao, H.; O'Connor, A. B.; Roveto, P.; Bauer, D.; Graceffa, R.; Richards, W. G.; Babij, P. *Bioorg. Med. Chem. Lett.* **2009**, 19, 4924.
- Han, S.; Mistry, A.; Chang, J. S.; Cunningham, D.; Griffor, M.; Bonnette, P. C.; Wang, H.; Chrnyk, B. A.; Aspnes, G. E.; Walker, D. P.; Brosius, A. D.; Buckbinder, L. *J. Biol. Chem.* **2009**, 284, 13193.
- Regan, J.; Pargellis, C. A.; Cirillo, P. F.; Gilmore, T.; Hickey, E. R.; Peet, G. W.; Proto, A.; Swinamer, A.; Moss, N. *Bioorg. Med. Chem. Lett.* **2009**, 19, 4924.
- For references on optimal drug-like properties see: (a) Bickerton, G. R.; Paolini, G. V.; Besnard, J.; Mureasan, S.; Hopkins, A. L. *Nat. Chem.* **2012**, 4, 90; (b) Gleeson, M. P.; Hersey, A.; Montanari, D.; Overington, J. *Nat. Rev. Drug Disc.* **2011**, 10, 197; (c) Hughes, J. D.; Blagg, J.; Price, D. A.; Bailey, S.; DeCrescenzo, G. A.; Devraj, R. V.; Elsworth, E.; Fobian, Y. M.; Gibbs, M. E.; Gilles, R. W.; Greene, N.; Huang, E.; Krieger-Burke, T.; Loesel, J.; Wager, T.; Whiteley, L.; Zhang, Y. *Bioorg. Med. Chem. Lett.* **2008**, 4872; (d) Leeson, P. D.; Springthorpe, B. *Nat. Rev. Drug Disc.* **2007**, 881; (e) Lipinski, C. A.; Lombardo, F.; Dominy, B. W.; Feeney, P. J. *Adv. Drug Deliv. Rev.* **1997**, 23, 3.
- Bonnette, P. C.; Robinson, B. S.; Silva, J. C.; Stokes, M. P.; Brosius, A. D.; Baumann, A.; Buckbinder, L. *J. Proteomics* **2010**, 73, 1306.
- Obach, R. S. *Drug Metab. Dispos.* **1999**, 27, 1350.
- Greengrass, P. M.; Stewart, M.; Wood, C. M. PCT WO 2003021271, March 13, 2003.
- Slack-Davis, J. K.; Martin, K. H.; Tighman, R. W.; Iwanicki, M.; Ung, E. J.; Autry, C.; Luzzio, M. J.; Cooper, B.; Kath, J. C.; Roberts, W. G.; Parson, J. T. *J. Biol. Chem.* **2007**, 282, 14845.
- Edwards, M. P.; Price, D. A. *Annu. Rep. Med. Chem.* **2010**, 45, 380. LipE values reported here were calculated using cLogD (at pH 7.4).
- Also referred to as LLE: Leeson, P. D.; Springthorpe, B. *Nat. Rev. Drug Disc.* **2007**, 881.
- Synthesis of **13j** (PF-4594755) has been published. See Ref. 13.
- The coordinates for crystal structures of PYK2 with pyrazole **13a** and indole **10c** have been deposited to PDB with accession codes 4H1J and 4H1M respectively.
- Kinase selectivity determined by a panel of biochemical kinase assays run in a 384-well streptavidin capture (flashplate) format in presence of a specific biotinylated peptide and a mixture of both unlabeled and ³³P-labeled ATP (assay run at K_m of ATP for each kinase).
- Guimarães, C. R.; Cardozo, M. J. *Chem. Inf. Model.* **2008**, 48, 958.